


Communication

# A Flexible Chemosensor Based on Colorimetric and Fluorescent Dual Modes for Rapid and Sensitive Detection of Hypochlorite Anion

Qin Wu <sup>1</sup>, Tao Tao <sup>1,2,\*</sup> , Yunxia Zhao <sup>1</sup> and Wei Huang <sup>2</sup>

<sup>1</sup> Institute of Advanced Materials and Flexible Electronics (IAMFE), School of Chemistry and Materials Science, Nanjing University of Information Science & Technology (NUIST), Nanjing 210044, China; 20191213038@nuist.edu.cn (Q.W.); nlgzyx@nuist.edu.cn (Y.Z.)

<sup>2</sup> School of Chemistry and Chemical Engineering, Nanjing University, Nanjing 210093, China; whuang@nju.edu.cn

\* Correspondence: taotao@nuist.edu.cn

**Abstract:** A flexible chemosensor has been developed based on colorimetric and fluorescent dual modes using tetraphenylethylene-centered tetraaniline (TPE4A) for rapid and sensitive detection of hypochlorite anion. The fluorescent probe TPE4A exhibits a unique aggregation-induced emission (AIE) character which is proved by a blue shift of the fluorescent peak from 544 to 474 nm with the water equivalents increasing. With the addition of hypochlorite in solution, the absorbance of the probe changes and the responding fluorescence color can be observed to change from light green to purple. The detection limit of hypochlorite is  $1.80 \times 10^{-4}$  M in solution, and the visual detection limit is  $1.27 \mu\text{g}/\text{cm}^2$  with the naked eye for the flexible paper-based chemosensor. The proposed flexible chemosensors show a good selectivity and sensitivity which has great potential for effective detection of hypochlorite anions without any spectroscopic instrumentation.

**Keywords:** aggregation-induced emission; chemosensor; tetraphenylethylene; hypochlorite; test paper



**Citation:** Wu, Q.; Tao, T.; Zhao, Y.; Huang, W. A Flexible Chemosensor Based on Colorimetric and Fluorescent Dual Modes for Rapid and Sensitive Detection of Hypochlorite Anion. *Sensors* **2021**, *21*, 8082. <https://doi.org/10.3390/s21238082>

Academic Editors: Ambra Giannetti, Mara Mirasoli and Sara Tombelli

Received: 15 November 2021

Accepted: 1 December 2021

Published: 3 December 2021

**Publisher's Note:** MDPI stays neutral with regard to jurisdictional claims in published maps and institutional affiliations.



**Copyright:** © 2021 by the authors. Licensee MDPI, Basel, Switzerland. This article is an open access article distributed under the terms and conditions of the Creative Commons Attribution (CC BY) license (<https://creativecommons.org/licenses/by/4.0/>).

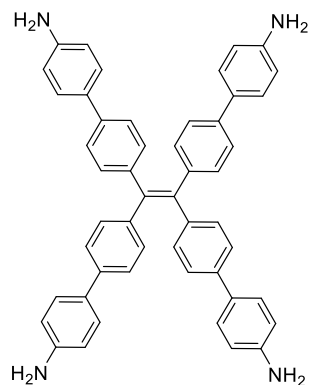
## 1. Introduction

Hypochlorite anion ( $\text{ClO}^-$ ) plays an essential role in biological organisms and environmental monitors, which not only is produced by  $\text{H}_2\text{O}_2$  and chloride ions in activated neutrophils [1–5] but is also a kind of disinfectant which can kill the coronavirus [6–8]. However, excessive hypochlorite could lead to diseases and even cancer including cardiovascular diseases, neuron degeneration, and arthritis [9,10]. Therefore, quantitative detection of hypochlorite with highly sensitive and selective methods becomes more and more crucial.

Many various analytical methods are available for the detection of hypochlorite (for example, colorimetric and fluorescent chemosensors) [11,12]. Recent reviews have summarized the advances of hypochlorite probes [13,14]. There are some successful designs for quantitative detection of hypochlorite based on the principle of colorimetric, chromatographic, electrochemical, and luminescent methods. Specifically, the fluorescent probe is a promising method with advantages such as low cytotoxicity, high selectivity, and fast response time for  $\text{ClO}^-$  detection. Moreover, understanding visual detection is an unceasingly thorough process for rapid and sensitive detection of hypochlorite anions [15–24].

Recently, dual modes [25–27] bioanalysis has become a popular research area, wherein researchers are studying scramble as well. When the environment changes in the direction of complexity, single-switch optical detection may no longer meet the reliability of data and the diversity of application scenarios. Therefore, it is very important to construct a dual-mode optical detection method. The optical detection based on colorimetric and fluorescent dual modes could not only improve the accuracy of results but also lead to

higher efficiency. In recent years, flexible thin-film devices [28,29] have been developed vigorously, especially in material, chemical, biological, physical fields, due to their unique advantages such as their low-cost, porosity, ready availability, mechanical flexibility, etc. Therefore, the design of paper-based chemosensors for simple and rapid detection is of great significance. In this work, we present a commercially available material **TPE4A** for fabricating a flexible paper-based chemosensor based on colorimetric and fluorescent dual modes in Scheme 1.



**Scheme 1.** The chemical structure of tetraphenylethylene-functionalized molecule **TPE4A**.

## 2. Results and Discussion

### 2.1. NMR Spectra

A commercially available material **TPE4A**, namely 4',4''',4''''',4''''''-(ethene-1,1,2,2-tetrayl)-tetrakis((1,1'-biphenyl)-4-amine) [30,31], has been purchased where the tetraphenylethylene (TPE) group shows an aggregation-induced emission (AIE) character [32,33]. The chemical structure of **TPE4A** has double checked by NMR spectra in Figure S1.  $^1\text{H}$  NMR (400 MHz,  $d^6$ -DMSO):  $\delta$  7.37 (d,  $J = 8.3$  Hz, 8H, TPE), 7.34 (d,  $J = 8.4$  Hz, 8H, Phenyl), 7.03 (d,  $J = 8.3$  Hz, 8H, TPE), 6.59 (d,  $J = 8.4$  Hz, 8H, Phenyl), 5.22 (s, 8H,  $\text{NH}_2$ ).

### 2.2. Aggregation-Induced Fluorescent Behavior

With the enhancement of volume fraction of water phase ( $f_w$ ), UV-Vis and fluorescent spectra have been shown for compound **TPE4A** in Figure 1. A step-by-step fluorescent turn-on is observed from  $f_w = 0$  to 70%, due to the controlled rotational motion in the molecule. Interestingly, a remarkable color change occurs from orange when  $f_w = 70\%$  to green when  $f_w = 80\%$  mainly due to the formation of aggregates. Simultaneously, the maximum emission wavelength  $\lambda_{\text{max}}$  is from 544 nm when  $f_w = 70\%$  to 474 nm when  $f_w = 80\%$ . Absorption and emission spectra show a clear AIE character for compound **TPE4A** as expected. The dominant luminescence is from the emissive solution to solid fluorescence. The same phenomenon is observed in the different concentration measurements. According to restriction of intramolecular vibrations (RIV) and restriction of intramolecular rotations (RIR), the possess of twisted intramolecular charge transfer (TICT) also is blocked, resulting in decreasing red-shift and increasing blue-shift.

### 2.3. Titration Experiment of Probe **TPE4A**

Compared to other chemical anions, molecule **TPE4A** has been designed as a highly selective fluorescent probe for  $\text{ClO}^-$  anion in Figure 2. After adding 1.00 mM of analytes, such as  $\text{SCN}^-$ ,  $\text{CO}_3^{2-}$ ,  $\text{S}^{2-}$ ,  $\text{NO}_2^-$ ,  $\text{H}_2\text{O}_2$ ,  $\text{F}^-$ , and  $\text{ClO}^-$ , UV-Vis absorption, and fluorescent intensities of probe **TPE4A** (40  $\mu\text{M}$ ) have been shown in mixed solution ( $f_w = 80\%$ ). The absorption peak of **TPE4A** is from 398 nm to 429 nm (also from 3.12 eV to 2.89 eV) in the presence of  $\text{ClO}^-$ , which is consistent with the results of calculated energy gaps.

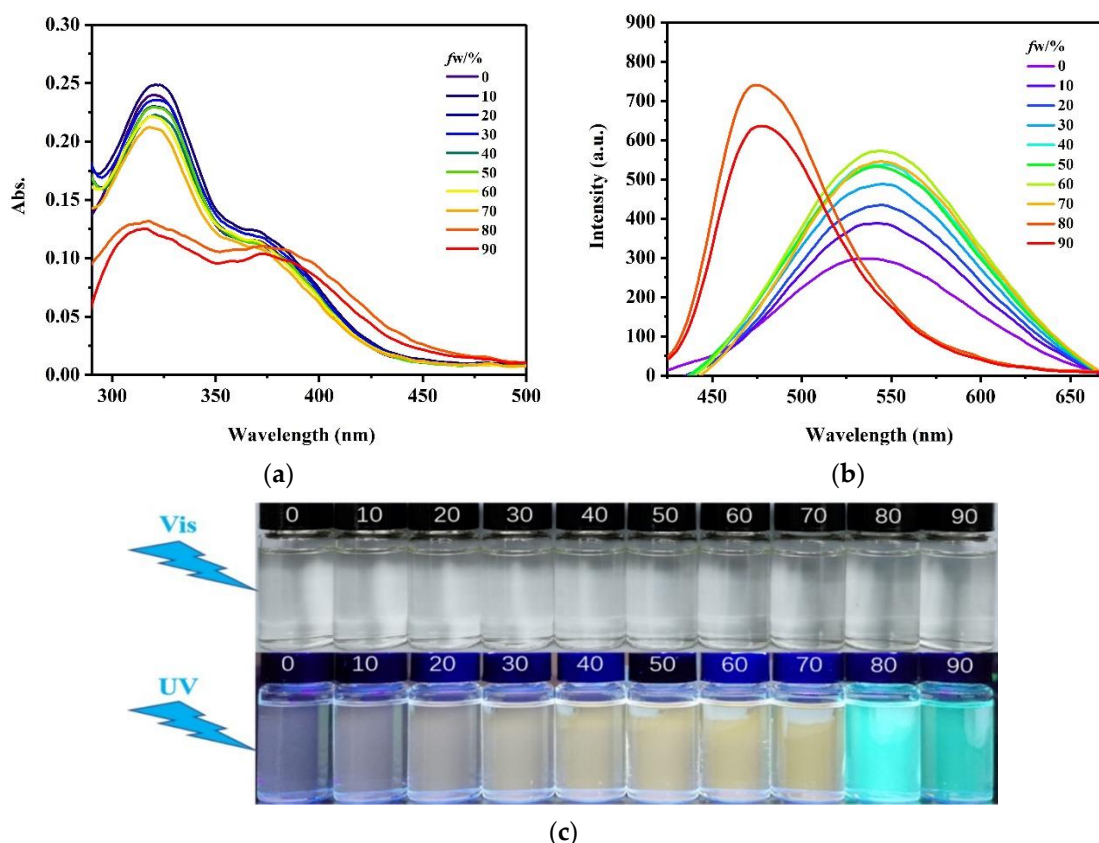


**Figure 1.** UV-Vis absorption (a) and fluorescent emission (b) spectra and their visual photograph (c) for compound TPE4A with different  $f_w$  in their THF/water solutions with the same concentration of 10  $\mu$ M.

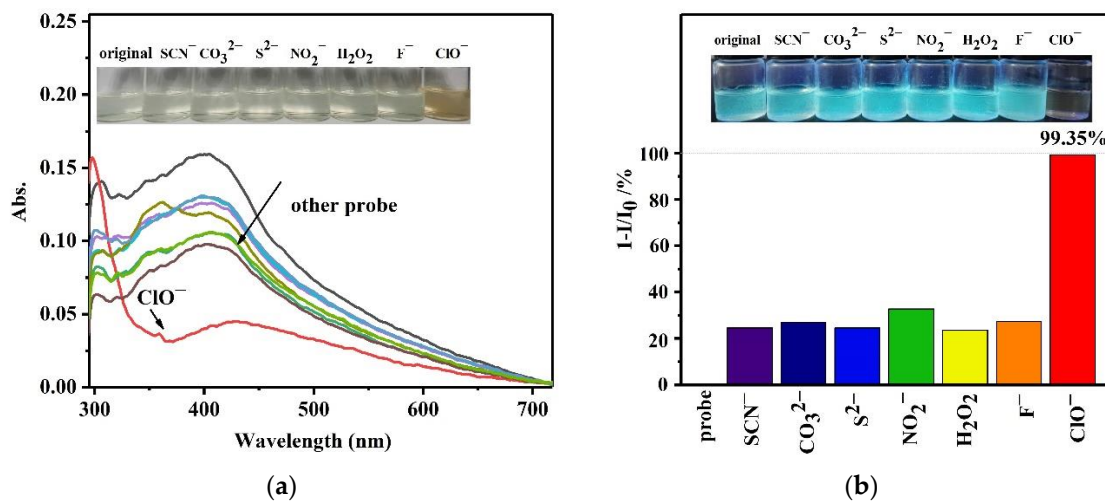


**Figure 2.** UV-Vis absorption (a) and fluorescent quenching percentages at 480 nm (b) of probe TPE4A (40  $\mu$ M) in mixed solution ( $f_w = 80\%$ ) upon exposure to other analytes for 60 s. Inset: a colorimetric and fluorescent change photograph for ClO<sup>-</sup> and other analytes (SCN<sup>-</sup>, CO<sub>3</sub><sup>2-</sup>, S<sup>2-</sup>, NO<sub>2</sub><sup>-</sup>, H<sub>2</sub>O<sub>2</sub>, and F<sup>-</sup>).

More importantly, a fluorescent quenching occurs from light green to dark, while the emissive color of this probe remains unchanged after the adding of other chemical species. Quantitative titration experiment shows a clear fluorescent turn-off in the presence of different concentrations of hypochlorite anion from 0 to 25 equivalent in mixed solution ( $f_w = 80\%$ ) with 100% of quenching percentage in Figure 3. It is noted that the intensity of

TPE4A at 480 nm does not significantly change under  $\text{H}_2\text{O}_2$  or  $\text{ClO}_4^-$  oxidants, since this compound avoids being oxidized in this case.

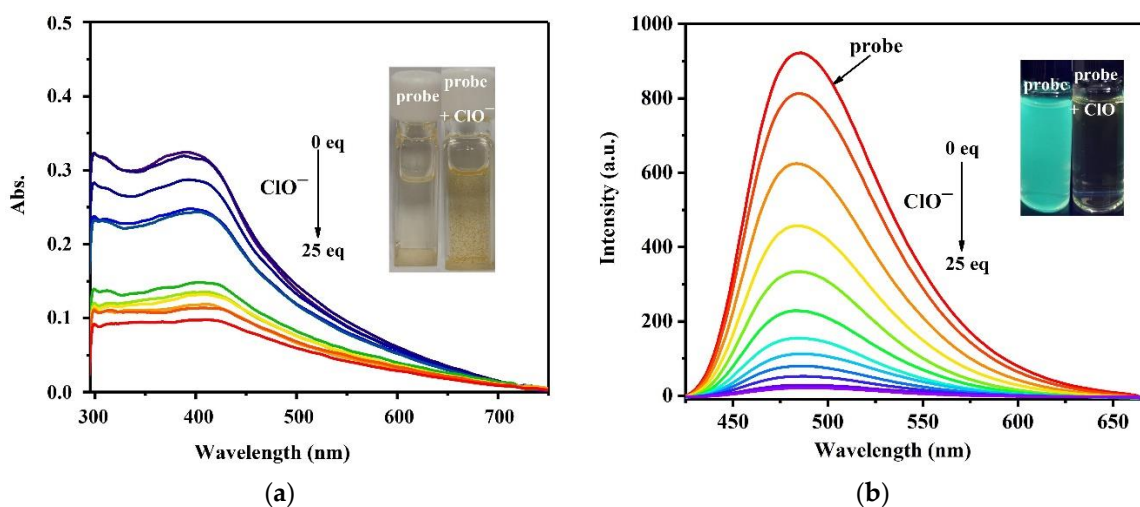


**Figure 3.** Absorption (a) and emission (b) titration spectra of the probe TPE4A (40  $\mu\text{M}$ ) in the presence of various concentrations of  $\text{ClO}^-$  from 0 to 25 equivalent in mixed solution ( $f_w = 80\%$ ). Inset: the contrastive pictures before and after the addition of  $\text{ClO}^-$ .

#### 2.4. Paper-Based Sensor

To effective detection of  $\text{ClO}^-$  in the state of aggregation, we prepared a test paper as the paper-based sensor. Then, we dipped the test paper into a solution containing chromophore test paper. As shown in Figure 4, the SEM diagram indicates that TPE4A can be attached to paper-based fibers. The diameter of particulate matter is approximately 100  $\mu\text{m}$ , while the diameter of melt-blown fibers is 20–50  $\mu\text{m}$ , showing a size matching on a micron scale. We carried out the naked-eye recognition matrix of paper-based sensor TPE4A for different concentrations of  $\text{ClO}^-$  under visible and UV light in Figure 5. The fluorescence of the paper-based sensor is quenched gradually with the increase of the concentration of  $\text{ClO}^-$ . At the same time, the color of the sensor changes from white to yellow under visible light, while from green to purple with the light of the UV lamp at 365 nm. Quantitative analysis demonstrates that the detection limit of hypochlorite is  $1.80 \times 10^{-4}$  M in solution based on the IUPAC definition 139 ( $C_{DL} = 3 \text{ Sb m}^{-1}$ ) [34], and the visual detection limit is 1.27  $\mu\text{g}/\text{cm}^2$  with the naked eye. Therefore, tetraphenylethylene-centered tetraaniline materials have a rapid and highly sensitive character for more convenient and visual detecting hypochlorite in a few seconds.

#### 2.5. Possible Mechanism of Probe TPE4A

According to the references [16,35,36], as well as experimental and theoretical calculations [37], we have investigated the possible mechanism of TPE4A in Scheme 2. First of all, the tetraaniline structure may be oxidized to the azo counterpart under an appropriate oxidant in this case. It is noted that perchloride is a stronger oxidant meant it could oxidize the aniline group to form the azo intermediate. However, the solubility of perchloride is limited in  $f_w = 80\%$ . The mechanism of fluorescent turn-off quenching is a reaction from strong chromophore TPE4A to weak chromophore TPE4A-NNCl, which could be speculated that owing to the oxidation of TPE4A. Furthermore, the C–N bond could be easy to cleavage in the azo intermediate and further to form a radical which could combine with chlorine radicals to form the compound TPE4A-NNCl. The energy gap is 3.44 eV for TPE4A, while the energy gap is 3.17 eV for TPE4A-NNCl (see Supporting Information).

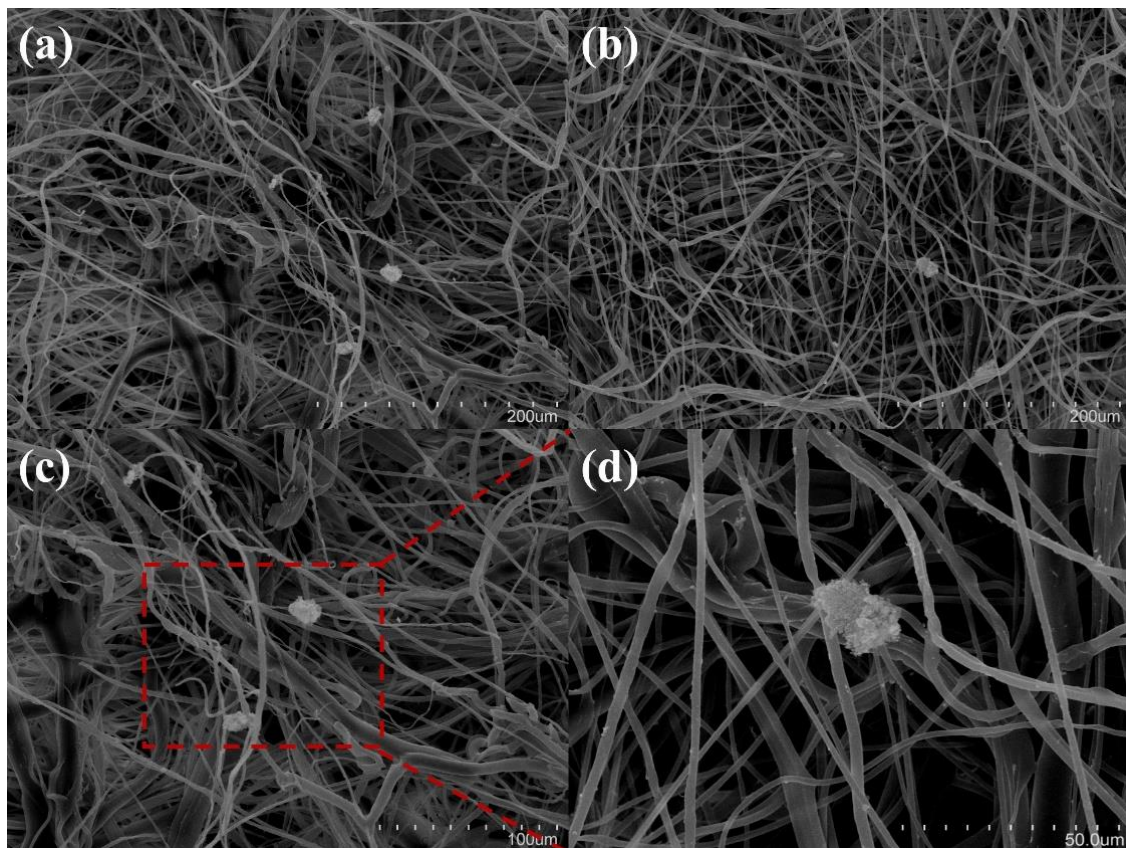


**Figure 4.** SEM images in different sizes of paper-based sensor TPE4A: 200  $\mu\text{m}$  (a,b), 100  $\mu\text{m}$  (c), and 50  $\mu\text{m}$  (d).

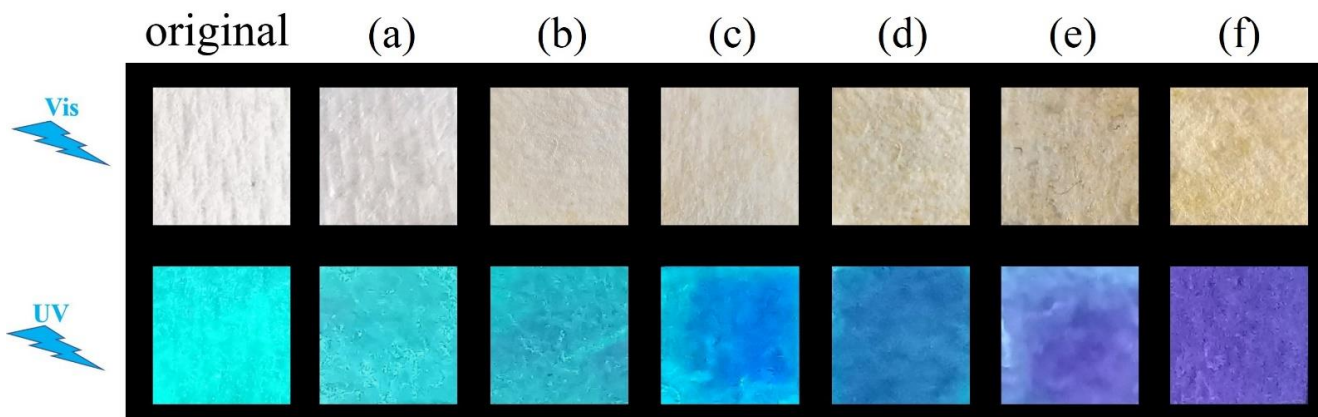
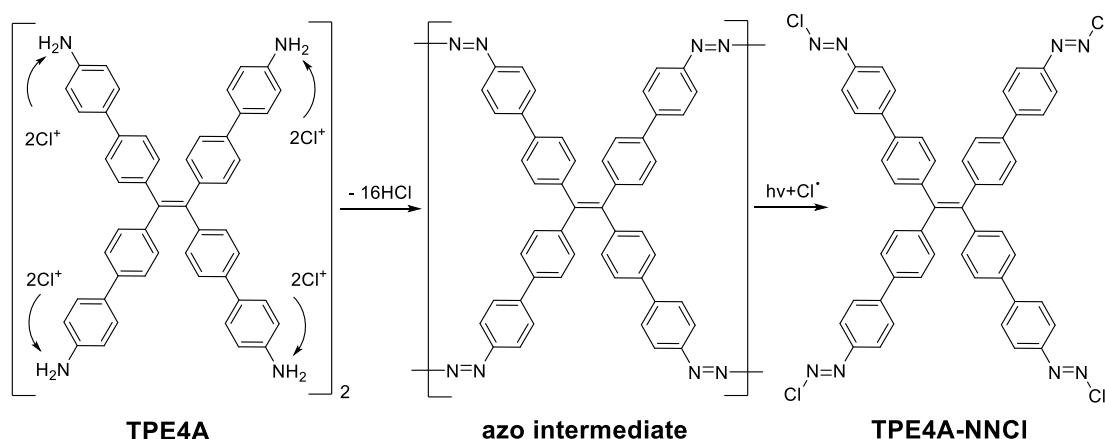


**Figure 5.** The naked-eye recognition matrix diagram of paper-based sensor TPE4A for different concentrations of  $\text{ClO}^-$  under visible and UV light. Original 0 M, (a)  $5.0 \times 10^{-4}$  M, (b)  $1.0 \times 10^{-3}$  M, (c)  $5.0 \times 10^{-3}$  M, (d)  $1.0 \times 10^{-2}$  M, (e)  $5.0 \times 10^{-2}$  M, (f)  $1.0 \times 10^{-1}$  M.

In addition, we carried out the ESI-MS analysis to explore the complete reaction mixture of the probe with  $\text{ClO}^-$  in Figure S3. ESI-MS analysis that a peak at  $m/z = 837.1954$  corresponding to  $[\text{TPE4A-NNCl-2Cl+Na}]^+$  (calcd for  $[\text{C}_{50}\text{H}_{32}\text{Cl}_2\text{N}_8\text{Na}]^+$ : 837.2019) is clearly observed with other identical isotopic peaks. This promoted a possible method to design fluorescent probes for hypochlorite with the inorganic/organic composites containing amino groups.



**Scheme 2.** Possible mechanism of chemosensor **TPE4A** for  $\text{ClO}^-$ .

### 3. Conclusions

In summary, we have designed and developed a flexible paper-based material for hypochlorite detection. The quantitative analysis demonstrates that with the enhancement of hypochlorite equivalents, the UV-Vis peaks have been decreasing from 398 nm to 429 nm, while the fluorescent peak at 480 nm has been decreasing more remarkably. Furthermore, the detection limit of hypochlorite is  $1.80 \times 10^{-4}$  M in solution, and the visual detection limit is  $1.27 \mu\text{g}/\text{cm}^2$  with the naked eye. The mechanism of fluorescent turn-off quenching is a reaction from strong chromophore **TPE4A** to weak chromophore **TPE4A-NNCI**, which has been confirmed by experimental and theoretical results, as well as support from references. This study can provide a flexible paper-based portable chemosensor based on colorimetric and fluorescent dual modes for hypochlorite before conventional chemical synthesis.

**Supplementary Materials:** The following are available online at <https://www.mdpi.com/article/10.3390/s21238082/s1>. Figure S1: <sup>1</sup>H NMR of **TPE4A**; Figure S2: The selectivity of **TPE4A** for  $\text{ClO}^-$ ,  $\text{SCN}^-$ ,  $\text{CO}_3^{2-}$ ,  $\text{S}^{2-}$ ,  $\text{NO}_2^-$ ,  $\text{H}_2\text{O}_2$ ,  $\text{F}^-$  and  $\text{ClO}_4^-$ ; Figure S3: Fitting plot for compound **1** with the addition of different contentions of **TPE4A** in THF solution to calculate the limit of detection; Figure S4: The experimental and theoretical ESI-MS of the product obtained by mixing probe NaOCl; Table S1: The HOMOs and LUMOs of compounds **TPE4A** and **TPE4A-NNCI**.

**Author Contributions:** Conceptualization, T.T.; methodology, Q.W.; formal analysis, Q.W. and T.T.; investigation, Q.W.; data curation, Q.W. and T.T.; writing—original draft preparation, Q.W. and T.T.; writing—review and editing, Y.Z. and W.H.; supervision, T.T. and Y.Z.; project administration, T.T.; funding acquisition, T.T. All authors have read and agreed to the published version of the manuscript.

**Funding:** This work was financially supported by the National Natural Science Foundation of China (No. 21501097), the Natural Science Foundation of Jiangsu Province (Nos. BK20150890 and BK20201389), Qing Lan Project of the Jiangsu Higher Education Institutions of China, and the Startup Foundation for Introducing Talent of NUIST (No. 2014R002) for financial aids.

**Institutional Review Board Statement:** Not applicable.

**Informed Consent Statement:** Not applicable.

**Data Availability Statement:** Not applicable.

**Conflicts of Interest:** The authors declare no conflict of interest.

### References

- Gross, S.; Gammon, S.T.; Moss, B.L.; Rauch, D.; Harding, J.; Heinecke, J.W.; Ratner, L.; Piwnica-Worms, D. Bioluminescence imaging of myeloperoxidase activity in vivo. *Nat. Med.* **2009**, *15*, 455–461. [[CrossRef](#)]
- Reja, S.I.; Bhalla, V.; Sharma, A.; Kaur, G.; Kumar, M. A highly selective fluorescent probe for hypochlorite and its endogenous imaging in living cells. *Chem. Commun.* **2014**, *50*, 11911–11914. [[CrossRef](#)]

3. Gui, S.L.; Huang, Y.Y.; Hu, F.; Jin, Y.L.; Zhang, G.X.; Yan, L.S.; Zhang, D.Q.; Zhao, R. Fluorescence turn-on chemosensor for highly selective and sensitive detection and bioimaging of Al<sup>3+</sup> in living cells based on ion-induced aggregation. *Anal. Chem.* **2015**, *87*, 1470–1474. [[CrossRef](#)] [[PubMed](#)]
4. Guo, Z.R.; Hu, T.L.; Sun, T.; Li, T.D.; Chi, H.; Niu, Q.F. A colorimetric and fluorometric oligothiophene-indenedione-based sensor for rapid and highly sensitive detection of cyanide in real samples and bioimaging in living cells. *Dyes Pigments* **2019**, *163*, 667–674. [[CrossRef](#)]
5. Xu, H.; Wu, S.L.; Lin, N.J.; Lu, Y.; Xiao, J.; Wang, Y.W.; Peng, Y. A NIR fluorescent probe for rapid turn-on detection and bioimaging of hypochlorite anion. *Sens. Actuators B Chem.* **2021**, *346*, 130484. [[CrossRef](#)]
6. Pattison, D.I.; Davies, M.J. Evidence for rapid inter- and intramolecular chlorine transfer reactions of histamine and carnosine chloramines: Implications for the prevention of hypochlorous-acid-mediated damage. *Biochemistry* **2006**, *45*, 8152–8162. [[CrossRef](#)]
7. Kohler, A.T.; Rodtoff, A.C.; Labahn, M.; Reinhardt, M.; Truyen, U.; Speck, S. Efficacy of sodium hypochlorite against multidrug-resistant Gram-negative bacteria. *J. Hosp. Inf.* **2018**, *100*, E40–E46. [[CrossRef](#)] [[PubMed](#)]
8. Chatterjee, A. Use of Hypochlorite Solution as Disinfectant during COVID-19 Outbreak in India: From the Perspective of Human Health and Atmospheric Chemistry. *Aerosol Air Qual. Res.* **2020**, *20*, 1516–1519. [[CrossRef](#)]
9. Wang, L.; Long, L.L.; Zhou, L.P.; Wu, Y.J.; Zhang, C.; Han, Z.X.; Wang, J.L.; Da, Z.L. A ratiometric fluorescent probe for highly selective and sensitive detection of hypochlorite based on the oxidation of *N*-alkylpyridinium. *RSC Adv.* **2014**, *4*, 59535–59540. [[CrossRef](#)]
10. Sun, Y.; Gao, Y.; Tang, C.; Dong, G.; Zhao, P.; Peng, D.; Wang, T.; Du, L.; Li, M. Multiple rapid-responsive probes towards hypochlorite detection based on dioxetane luminophore derivatives. *J. Pharm. Anal.* **2021**, in press. [[CrossRef](#)]
11. Jin, L.; Xu, M.Y.; Jiang, H.; Wang, W.L.; Wang, Q.M. A simple fluorescein derived colorimetric and fluorescent ‘off-on’ sensor for the detection of hypochlorite. *Anal. Methods* **2018**, *10*, 4562–4569. [[CrossRef](#)]
12. Dongare, P.R.; Gore, A.H. Recent advances in colorimetric and fluorescent chemosensors for ionic species: Design, principle and optical signalling mechanism. *ChemistrySelect* **2021**, *6*, 5657–5669. [[CrossRef](#)]
13. Ma, C.G.; Zhong, G.Y.; Zhao, Y.; Zhang, P.; Fu, Y.Q.; Shen, B.X. Recent development of synthetic probes for detection of hypochlorous acid/hypochlorite. *Spectrochim. Acta Part A Mol. Biomol. Spectrosc.* **2020**, *240*, 118545. [[CrossRef](#)]
14. Song, Z.-G.; Yuan, Q.; Lv, P.; Chen, K. Research progress of small molecule fluorescent probes for detecting hypochlorite. *Sensors* **2021**, *21*, 6326. [[CrossRef](#)]
15. Zhu, B.C.; Xu, Y.H.; Liu, W.Q.; Shao, C.X.; Wu, H.F.; Jiang, H.L.; Du, B.; Zhang, X.L. A highly selective colorimetric probe for fast and sensitive detection of hypochlorite in absolute aqueous solution. *Sens. Actuators B Chem.* **2014**, *191*, 473–478. [[CrossRef](#)]
16. Li, J.F.; Huo, F.J.; Yin, C.X. A selective colorimetric and fluorescent probe for the detection of ClO<sup>−</sup> and its application in bioimaging. *RSC Adv.* **2014**, *4*, 44610–44613. [[CrossRef](#)]
17. Yu, S.Y.; Hsu, C.Y.; Chen, W.C.; Wei, L.F.; Wu, S.P. A hypochlorous acid turn-on fluorescent probe based on HOCl-promoted oxime oxidation and its application in cell imaging. *Sens. Actuators B Chem.* **2014**, *196*, 203–207. [[CrossRef](#)]
18. Venkatesan, P.; Wu, S.P. A turn-on fluorescent probe for hypochlorous acid based on the oxidation of diphenyl telluride. *Analyst* **2015**, *140*, 1349–1355. [[CrossRef](#)]
19. Chen, W.C.; Venkatesan, P.; Wu, S.P. A highly selective turn-on fluorescent probe for hypochlorous acid based on hypochlorous acid-induced oxidative intramolecular cyclization of boron dipyrromethene-hydrazone. *Anal. Chim. Acta* **2015**, *882*, 68–75. [[CrossRef](#)]
20. Zhu, H.; Zhang, Z.; Long, S.R.; Du, J.J.; Fan, J.L.; Peng, X.J. Synthesis of an ultrasensitive BODIPY-derived fluorescent probe for detecting HOCl in live cells. *Nat. Protoc.* **2018**, *13*, 2348–2361. [[CrossRef](#)]
21. Hwang, S.M.; Kim, A.; Kim, C. A simple hydrazine-based probe bearing anthracene moiety for the highly selective detection of hypochlorite. *Inorg. Chem. Commun.* **2019**, *101*, 1–5. [[CrossRef](#)]
22. Hu, Y.; Liu, J.; You, X.; Wang, C.; Li, Z.; Xie, W. A light-up probe for detection of adenosine in urine samples by a combination of an AIE molecule and an aptamer. *Sensors* **2017**, *17*, 2246. [[CrossRef](#)]
23. Rha, C.J.; Lee, H.; Kim, C. Development of an azo-naphthol-based probe for detecting hypochlorite (ClO<sup>−</sup>) via color change in aqueous solution. *Inorg. Chem. Commun.* **2020**, *121*, 108244. [[CrossRef](#)]
24. Lee, S.C.; Park, S.; So, H.; Lee, G.; Kim, K.-T.; Kim, C. An acridine-based fluorescent sensor for monitoring ClO<sup>−</sup> in water samples and zebrafish. *Sensors* **2020**, *20*, 4764. [[CrossRef](#)]
25. Zhou, Y.Y.; Zhuang, Y.P.; Li, X.; Agren, H.; Yu, L.; Ding, J.D.; Zhu, L.L. Selective dual-channel imaging on cyanostyryl-modified azulene systems with unimolecularly tunable visible-near infrared luminescence. *Chem. Eur. J.* **2017**, *23*, 7642–7647. [[CrossRef](#)]
26. Fang, H.; Gan, Y.T.; Wang, S.R.; Tao, T. A selective and colorimetric chemosensor for fluoride based on dimeric azulene boronate ester. *Inorg. Chem. Commun.* **2018**, *95*, 17–21. [[CrossRef](#)]
27. Kim, D.; Jeong, K.; Kwon, J.E.; Park, H.; Lee, S.; Kim, S.; Park, S.Y. Dual-color fluorescent nanoparticles showing perfect color-specific photoswitching for bioimaging and super-resolution microscopy. *Nat. Commun.* **2019**, *10*, 3089. [[CrossRef](#)]
28. Zhu, Q.B.; Li, B.; Yang, D.D.; Liu, C.; Feng, S.; Chen, M.L.; Sun, Y.; Tian, Y.N.; Su, X.; Wang, X.M.; et al. A flexible ultrasensitive optoelectronic sensor array for neuromorphic vision systems. *Nat. Commun.* **2021**, *12*, 1798. [[CrossRef](#)]
29. Kim, S.; Yun, T.G.; Kang, C.; Son, M.J.; Kang, J.G.; Kim, I.H.; Lee, H.J.; An, C.H.; Hwang, B. Facile fabrication of paper-based silver nanostructure electrodes for flexible printed energy storage system. *Mater. Des.* **2018**, *151*, 1–7. [[CrossRef](#)]

30. Jiao, J.J.; Li, Z.J.; Qiao, Z.W.; Li, X.; Liu, Y.; Dong, J.Q.; Jiang, J.W.; Cui, Y. Design and self-assembly of hexahedral coordination cages for cascade reactions. *Nat. Commun.* **2018**, *9*, 4423. [[CrossRef](#)]
31. Liu, Y.Z.; Diercks, C.S.; Ma, Y.H.; Lyu, H.; Zhu, C.H.; Alshimri, S.A.; Alshihri, S.; Yaghi, O.M. 3D covalent organic frameworks of interlocking 1D square ribbons. *J. Am. Chem. Soc.* **2019**, *141*, 677–683. [[CrossRef](#)]
32. Huang, L.; Tao, H.; Zhao, S.J.; Yang, K.; Cao, Q.Y.; Lan, M.H. A tetraphenylethylene-based aggregation-induced emission probe for fluorescence turn-on detection of lipopolysaccharide in injectable water with sensitivity down to picomolar. *Ind. Eng. Chem. Res.* **2020**, *59*, 8252–8258. [[CrossRef](#)]
33. Zhang, S.S.; Huang, Y.P.; Kong, L.; Zhang, X.J.; Yang, J.X. Aggregation-induced emission-active tetraphenylethylene derivatives containing arylimidazole unit for reversible mechanofluorochromism and selective detection of picric acid. *Dyes Pigments* **2020**, *181*, 108574. [[CrossRef](#)]
34. Ding, Y.; Li, X.; Li, T.; Zhu, W.; Xie, Y.  $\alpha$ -Monoacylated and  $\alpha,\alpha'$ - and  $\alpha,\beta'$ -diacylated dipyrins as highly sensitive fluorescence “turn-on”  $\text{zn}^{2+}$  probes. *J. Org. Chem.* **2013**, *78*, 5328–5338. [[CrossRef](#)]
35. Xiong, K.M.; Huo, F.J.; Yin, C.X.; Chu, Y.Y.; Yang, Y.T.; Chao, J.B.; Zheng, A.M. A novel recognition mechanism supported by experiment and theoretical calculation for hypochlorites recognition and its practical application. *Sens. Actuators B Chem.* **2016**, *224*, 307–314. [[CrossRef](#)]
36. Cheng, X.H.; Jia, H.Z.; Long, T.; Feng, J.; Qin, J.G.; Li, Z. A “turn-on” fluorescent probe for hypochlorous acid: Convenient synthesis, good sensing performance, and a new design strategy by the removal of C=N isomerization. *Chem. Commun.* **2011**, *47*, 11978–11980. [[CrossRef](#)]
37. Frisch, M.J.; Trucks, G.W.; Schlegel, J.; Scuseria, G.E.; Robb, M.A.; Cheeseman, J.R.; Schlegel, H.B.; Scalmani, G.; Barone, V.; Mennucci, B.; et al. *Gaussian 09, Revision C.01*; Gaussian, Inc.: Wallingford, CT, USA, 2010.